

# Confirming correctness of procedure for determining soft parameters in Coulomb potential of noble atoms

Thu D. H. Truong\*, Bach N. X. Ho, Tai V. Do

Department of Physics, Ho Chi Minh City University of Education, Ho Chi Minh City, Viet Nam

\* Correspondence to Thu D. H. Truong <thutdh@hcmue.edu.vn>

(Received: 08 March 2024; Revised: 29 March 2024; Accepted: 29 March 2024)

**Abstract.** This paper verifies that the procedure described in [Computer Physics Communications, 276, 108372 (2022)] for determining the soft parameters in the Coulomb potential of noble atoms is accurate via the modification of the initial position value of  $x_0$  and the parameter  $b$  range. In the case of nonsequential double ionization (NSDI), the results demonstrate that the value of  $x_0$  is not contingent upon the range of computed parameter  $a$ . Furthermore, we examine the significance of parameter  $b$  in the NSDI process and conclude that the ideal value for the soft Coulomb parameter of  $b$  is that  $b \leq 0.1$  a.u.

**Keywords:** soft parameter, Coulomb potential, nonsequential double ionization, classical model

## 1 Introduction

One of the most fundamental processes that can occur in the interaction of an atom or a molecule with a strong electric field is nonsequential double ionization (NSDI) [1–8]. Since the initial observation of the enhanced double ionization (DI) yield of noble gases [9], numerous scientists have been intrigued by the NSDI process. Ascertained through the measurement of an electron or ion's momentum, NSDI is attributed to the widely recognized phenomenon of recollision [10]. The initial electron that undergoes ionization via tunneling is driven back to the parent ion when the electric field reverses its direction and an inelastic recollision expels the second electron.

There are currently three prevalent approaches to NSDI. The initial approach involves quantum considerations, specifically the utilization of a laser field to solve the time-dependent Schrödinger equation (TDSE) to acquire electron ionization information. The second method employs a semi-classical

approach, wherein the ionization process of the atom is described by using the approximative ADK (Ammosov-Delone-Krainov) method [11], while the trajectory of ionized electrons in the laser field is regarded as a classical phenomenon. The third approach entails treating electrons as entities entirely governed by the principles of classical physics. The classical method, initially introduced by Panfili in 2001 [12], has been extensively implemented. Its primary benefit is that it permits the examination of the electron state at any given moments throughout the laser field interaction. In addition, it has been demonstrated that this method is as precise as the TDSE method when the laser intensity is sufficiently high to induce ionization through the barrier mechanism, and the system particle count is sufficient to minimize statistical errors [13].

The Coulomb potential of the nucleus complicates calculations with the classical method because of the instability of this model, caused by the autoionization of the binding electrons [13]. Consequently, to circumvent autoionization and

the singularity of the Coulomb potential, researchers consider the soft Coulomb potential. This method is extensively employed in rigorous field research because of its lack of impact on the physical characteristics of the process [12, 14, 15]. The fact that the soft parameters of Coulomb potential are unique to each atom or molecule is intriguing. Thu et al. introduced a method for ascertaining the soft parameters in the Coulomb potential of noble atoms [16], which utilized the classical ensemble model and included the soft parameter  $a$  and initial position  $x_0$ .

Following this, the kinetic energy of every atom was arbitrary allocated between two electrons, with each electron's initial motion being determined in a random direction. Prior to activating the laser, the ensemble was permitted to evolve autonomously for approximately 200 a.u. to acquire stable momentum and position distributions. Upon the conclusion of free evolution, it was anticipated that the electrons within each atom would be constrained by two factors: they must possess negative energies and be situated in close proximity to the ion core. The authors simulated the ratio of double-to-single ionization counts as a function of intensity, correlated two-electron momentum distributions (CTEMD) in the NSDI process for the atom, and compared them with experimental works to determine the optimal value parameters  $a$  and  $x_0$ . Furthermore, the soft parameter  $b$  remained constant in [16] throughout the derivation process of  $a$  and  $x_0$ . The authors posited that there existed a relationship between the value of parameter  $b$  and the probability of a recollision process. Furthermore, Wang [17] examined the likelihood of self-ionization as a function of  $b$  between 0 and 10 a.u. and then drew a conclusion regarding the value of parameter  $a$ . However, previous researchers had not extensively examined the function of parameter  $b$  or its impact on the NSDI process simulation.

By employing the classical three-dimensional ensemble model, we expanded the range of investigation for the initial position  $x_0$  to ascertain parameter  $a$  in this article. Furthermore, to examine the role of parameter  $b$ , we conducted simulations of the NSDI process utilizing various values of the  $b$  parameter. We, hereby, validated the precision of the method described in [16].

## 2 Method

The classical method is widely used in the NSDI process. In this model, the motion of two electrons is governed by Newton's equation:

$$\frac{d^2\vec{r}_i}{dt^2} = -\vec{\nabla}[U_{ne}(r_i) + U_{ee}(r_1, r_2)] + \vec{F}(t), \quad (1)$$

where  $i$  is the label of two electrons;  $\vec{r}_i$  is the coordinate of the  $i$ th electron; and  $\vec{F}(t)$  is the force of the electric field. The ion-electron attractive potential and the electron-electron ( $e-e$ ) repulsive potential are  $U_{ne}(\vec{r}_i) = -2/\sqrt{r_i^2 + a^2}$

and

$$U_{ee}(\vec{r}_1, \vec{r}_2) = 1/\sqrt{(r_1 - r_2)^2 + b^2},$$

respectively, where  $a, b$  are the soft parameters to prevent autoionization of Coulomb interaction.

In Ref. [16], the authors proposed a procedure to determine the soft parameters of the Coulomb potential in which parameter  $b$  was fixed during the investigation. To confirm the accuracy of the procedure in Ref. [16], we performed steps (i) and (ii) in this report with different values of  $b$  and  $x_0$ . From pairs of parameters  $(a, x_0)$ , we proceeded to simulate the NSDI process:

(i) We determined the initial state of the atomic system from equation (1) in the absence of the laser field. For the Ar atom, the initial conditions were obtained when the system was in

the ground state with the energy value of  $-1.5911$  a.u. (the total ionization energy of the first and the second electrons). The available kinetic energy of the two electrons was randomly distributed between them in the momentum space. To obtain a stable momentum and position distribution of the system, the electrons were moved in the atomic nuclear field for a sufficiently long time (200 a.u.).

(ii) We solved equation (1) for each atom in the presence of the laser electric field. At the end of the interaction, the energy of each electron consisted of the kinetic energy, the ion-electron interaction potential, and the half electron-electron interaction potential. After the interaction of the atom with the laser electric field, a DI event was defined if the two-electron energy value was positive. To reduce statistical errors and obtain stable results, we examined a set of 4.000.000 atoms.

Finally, we analysed and confirmed the accuracy of the procedure.

### 3 Results and discussion

To verify the influence of the initial position range  $x_0$  on parameter  $a$ , we proceeded to examine step (i) in [16] using various value ranges of  $x_0$ . Fig. 1 illustrates the minimum values of the second electron's potential (green dashed) and the total potential (red solid) energies for  $x_0$  between  $-5$

and  $5$  a.u. (a) and  $-7$  and  $7$  a.u.; (b) as a function of parameter  $a$ . The horizontal solid blue lines represent the combined ground-state energies of the neutral atom Ar and the ion  $\text{Ar}^+$  ( $E_p$ ), as observed. The view is guided by the vertical dash-dotted black lines. The potential range of  $a$ , as indicated in the data presented in Figs. 1a and 1b and contingent upon the conditions in [16], is from  $1.25$  to  $1.62$  a.u. This outcome is entirely consistent with that of the previous research [16].

Then, the optimal value of the initial position was chosen at the minimum of the total potential  $U_{\text{total}}$  in Fig. 2. Note that to ensure the condition of the classical, the kinetic energy is positive, implying that  $\min[U_{\text{total}}|_{t=0}(x_0)] < E_p$ . The values of optimal  $x_0$  corresponding to each value of  $a$  for two different ranges of  $x_0$  are given in Table 1. Here, we compared initial position  $x_0$  in case of  $x_0 \in [-3\text{a.u.}; 3\text{a.u.}]$  for the possible values of  $a$  in Ref. [16] in the last row of Table 1.

The results demonstrate that the initial values of  $x_0$  did not change when different value ranges of  $x_0$  were investigated. Note that, our result is consistent with that in [16] regarding the values (see Figs. 2a–2h) and the analysis (see equation (14)). Therefore, we affirmed that the range of guess initial position  $x_0$  did not affect the determination of parameter  $a$  and the optimal value of  $x_0$  as the input parameters in the NSDI calculation.

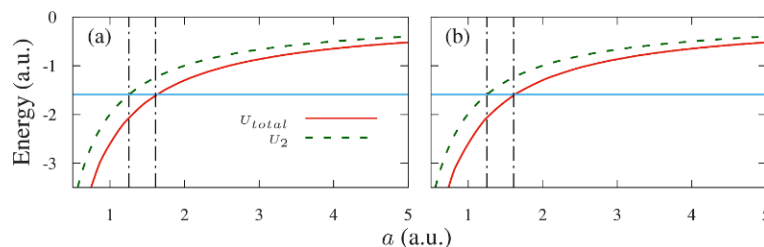


**Fig. 1.** Minimum value of total potential (red solid) and second electron's potential (green dashed) energies as functions of parameter  $a$  for  $x_0$ : (a) from  $-5$  to  $5$  a.u. and (b) from  $-7$  to  $7$  a.u.;  $b = 0.1$  a.u.

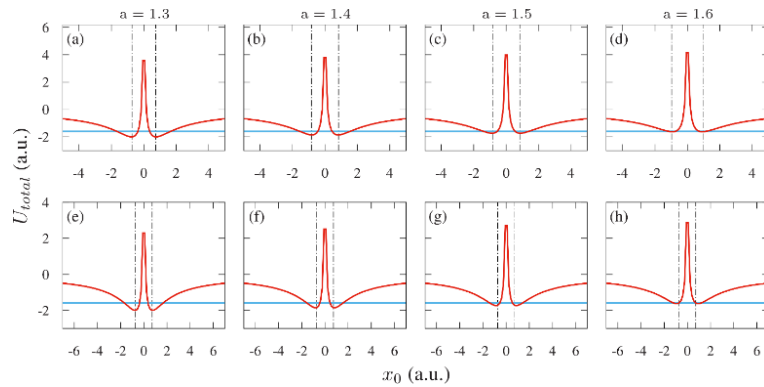


**Fig. 2.** Total potential energy as function of initial position  $x_0$  for four representative values of parameter  $a$ ;  $x_0$  from  $-5$  to  $5$  a.u. (a–d) and from  $-7$  to  $7$  a.u. (e–h);  $b = 0.1$  a.u.

**Table 1.** Soft parameter  $a$  and appropriately initial position for Ar atom;  $b = 0.1$

	$a$ (a.u.)	1.3	1.4	1.5	1.6
$x_0 \in [-5;5]$ (a.u.)	Optimal $x_0$ (a.u.)	0.74	0.80	0.86	0.94
$x_0 \in [-7;7]$ (a.u.)	Optimal $x_0$ (a.u.)	0.75	0.81	0.86	0.93
$x_0 \in [-3;3]$ (a.u.)	Optimal $x_0$ (a.u.)	0.75	0.80	0.86	0.92

In addition, as we know the real value of  $b$  is zero, in the classical model, soft parameter  $b$  can be chosen arbitrarily. However, a recollision is inefficient for a large  $b$ , leading to a decrease of the NSDI signals [16]. Previous works usually assumed that  $b \leq 0.1$  [14, 18–21]. Thus, to reconfirm the calculation procedure in [16], we present here the investigation when  $b = 0.05$  a.u. and  $x_0 \in [-3;3]$  a.u. in Fig. 3 for the operation of choosing a possible range of  $a$  and associating input  $x_0$ . Fig. 3a shows that the possible range of  $a$  is still between 1.25 and 1.62 a.u. Figs 3b–3e display the total potential energy as a function of the initial position  $x_0$  for four representative values of parameter  $a$ . The values of pairs  $(a, x_0)$  are given in Table 2.

**Table 2.** Soft parameter  $a$  and appropriately initial position for Ar atom;  $b = 0.05$  and  $x_0 \in [-3;3]$  a.u.]

$a$ (a.u.)	1.3	1.4	1.5	1.6
Optimal $x_0$ (a.u.)	0.75	0.81	0.87	0.92

In the next step, we simulated the NSDI process and showed the ratio of double to single

ionization counts of the Ar atom to pick up the optimal value of  $a$  in Fig. 3f. We focused on the influence of laser intensity on the NSDI of the atomic system. Thus, the trapezoidal laser pulse of the 780 nm wavelength and the total length of 10 optical cycles, including two turn-on cycles, six cycles at full strength, and two turn-off cycles, was considered. The equation of the laser pulse is

$$\vec{F}(t) = F_0 \sin(\omega t) f(t) \hat{i}, \quad (2)$$

where the envelope function has the following form

$$f(t) = \begin{cases} \frac{t}{N_1 T_0} & (0 \leq t \leq N_1 T_0) \\ 1 & (N_1 T_0 < t \leq (N_1 + N_2) T_0), \\ \frac{(N_1 + N_2 + N_3) T_0 - t}{N_3 T_0} & ((N_1 + N_2) T_0 < t) \end{cases} \quad (3)$$

where  $N_1 = 2$ ;  $N_2 = 6$ ;  $N_3 = 2$ ;  $T_0 = 2\pi/\omega$  is the optical cycle of the laser field. It is a surprise that the special “knee” structure appears only when  $a = 1.5$  a.u. at the intermediate laser intensities from  $I = 4.0 \times 10^{14}$  W/cm<sup>2</sup> to  $I = 5.0 \times 10^{14}$  W/cm<sup>2</sup>. The results are consistent with those in [16].

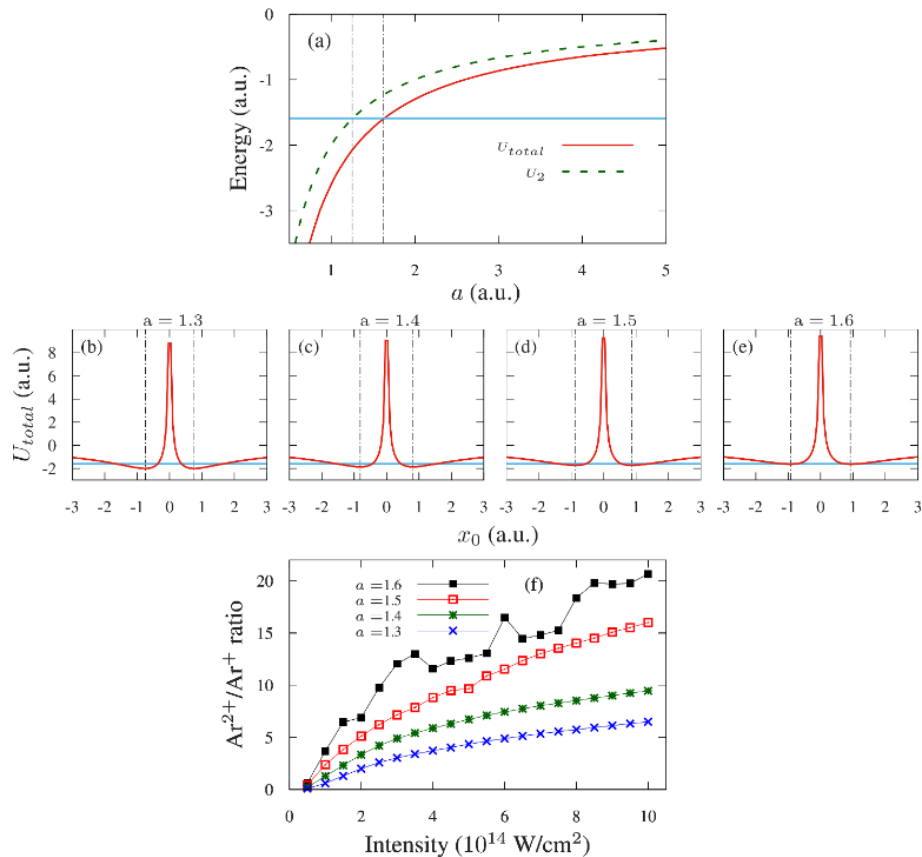


**Fig. 3.** (a) Minimum value of total potential (red solid) and second electron’s potential (green dashed) energies as functions of parameter  $a$ ; (b–e) Total potential energy as function of initial position  $x_0$  for four representative values of parameter  $a$ ; (f) Ratio of double-to-single ionization counts as function of intensity for Ar atom;  $x_0 \in [-3;3$  a.u.];  $b = 0.05$

Additionally, in his dissertation [17], Wang considered the probability of self-ionization as a function of  $b$  from 0 to 10 a.u., corresponding to several representative values of  $a$  in the range from 1 to 1.6 a.u. and pointed out that the best value of  $a$  for Ar was 1.5 a.u. since the self-ionization probability was almost zero. This result implies that the characteristic of the NSDI process should remain for any values of  $b$ . To confirm this evidence, Fig. 4 shows the minimum value of the total potential and the second electron’s potential energies as functions of parameter  $a$  and the ratio of double-to-single ionization counts as a function of intensity for the Ar atom when  $b = 1$  a.u. (the first column),  $b = 2$  a.u. (the second column), and  $x_0 \in [-3;3$  a.u.]. The result shows that the possible range of  $a$  extends when increasing the value of parameter  $b$  (see Fig.s 4a–b). Moreover, the values

of pairs  $(a, x_0)$  are different in Table 1 and Table 2. Even if  $b = 2$  a.u., the value of  $x_0$  in equation (14) in Ref. [16] is still unknown. In addition, the result demonstrates that the characterized “knee structure” totally disappears when  $b = 1$  a.u. and  $b = 2$  a.u., indicating that we cannot use large values of  $b$  to keep the physical characteristic of NSDI process.

Finally, we examined the CTEM in the direction parallel to the laser polarization for a comparison with experimental results of Eremina et al. [22] when  $a = 1.5$  a.u. with different values of  $b$  in Fig. 5. According to Ref. [22], for the moderate intensity of  $I = 1.5 \times 10^{14}$  W/cm<sup>2</sup>, the CTEM displays a clear double-line structure, which is parallel to the main diagonal. In which, in the case when  $I = 0.9 \times 10^{14}$  W/cm<sup>2</sup>, the CTEM exhibits

equal distribution into four quarters. Fig. 5 indicates that our simulation is consistent with the experimental data [22] when  $b = 0.1$  a.u. (see Figs. 5a and 5d). In addition, when the value of  $b$  increases, the number of DI events significantly decreases. In our calculation, in case when  $b = 2$

a.u., these DI events account for approximately  $3.25 \times 10^{-4} \%$  when  $I = 0.9 \times 10^{14} \text{ W/cm}^2$  and  $1.18 \times 10^{-3} \%$  when  $I = 1.5 \times 10^{14} \text{ W/cm}^2$ . The result again confirms that the optimal value for the soft Coulomb parameter is that  $b \leq 0.1$  a.u.

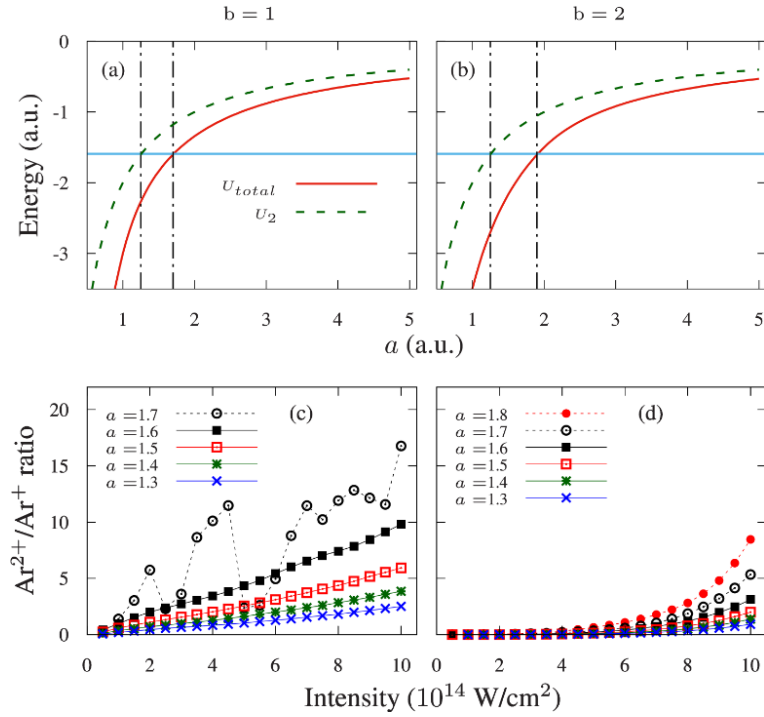


**Fig. 4.** (a, c) Minimum value of total potential (red solid) and second electron's potential (green dashed) energies as functions of parameter  $a$ ; (b, d) Ratio of double-to-single ionization counts as function of intensity for Ar atoms.  $x_0 \in [-3; 3$  a.u.];  $b = 1$  a.u. (the first column);  $b = 2$  a.u. (the second column)

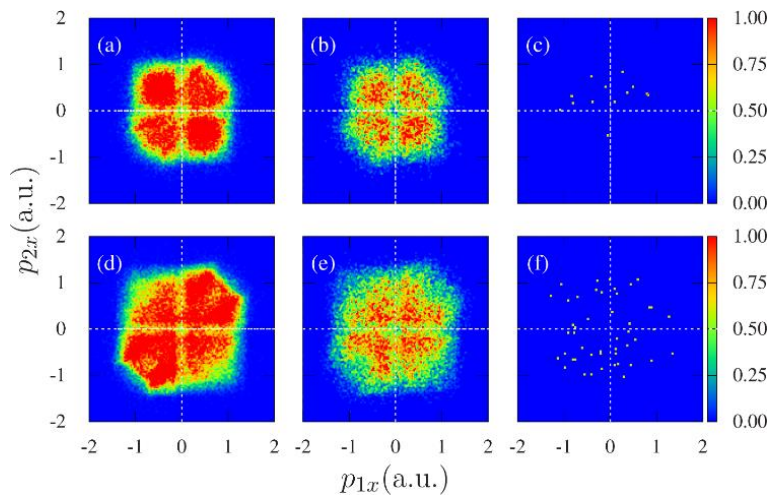


**Fig. 5.** Correlated two-electron momentum distributions in NSDI process of Ar atoms for two representative laser intensities  $0.9 \times 10^{14} \text{ W/cm}^2$  (top row) and  $1.5 \times 10^{14} \text{ W/cm}^2$  (bottom row) when  $a = 1.5$  a.u. and different values of  $b$ :  $b = 0.1$  a.u. (a, d);  $b = 1$  a.u. (b, e) and  $b = 2$  a.u. (c, f). The laser wavelength is 780 nm

## 4 Conclusion

In this paper, we extended the value range of the initial position  $x_0$  and investigated the role of parameter  $b$  in the simulation NSDI process by employing the traditional three-dimensional ensemble model, comparing the research findings with those in theoretical and experimental works. This demonstrates the precision of the method utilized in Ref. [16] to ascertain that the soft parameters in the Coulomb potential,  $x_0$  and  $b$ , are varied.

## References

1. Rudenko A, de Jesus VLB., Ergler Th, Zrost K, Feuerstein B, Schröter CD, et al. Correlated two-electron momentum spectra for strong-field nonsequential double ionization of He at 800 nm. *Physical Review Letters*. 2007;99:263003.
2. Hao X, Li W, Liu J, Chen J. Effect of the electron initial longitudinal velocity on the nonsequential double-ionization process. *Physical Review A*. 2011;83:053422.
3. Bergues B, Kübel M, Johnson NG, Fischer B, Camus N, Betsch KJ, et al. Attosecond tracing of correlated electron-emission in non-sequential double ionization. *Nature Communications*. 2012;3:813.
4. Emmanouilidou A, Meltzer T. Recollision as a probe of magnetic field effects in non-sequential double ionization. *Physical Review A*. 2017;95:033405.
5. Sun F, Chen X, Zhang W, Qiang J, Li H, Lu P, et al. Longitudinal photon-momentum transfer in strong-field double ionization of argon atoms. *Physical Review A*. 2020;101:021402.
6. Chen Z, Zhou A, Morishita T, Bai Y, Hao X, Zatsarinny O, et al. Anticorrelation in nonsequential double ionization of helium. *Physical Review A*. 2021; 103:053102.
7. Hao X, Bai Y, Li C, Zhang J, Li W, Yang W, et al. Recollision of excited electron in below-threshold nonsequential double ionization. *Communications Physics*. 2022;5:31.
8. Truong TDH, Tran DAT, Nguyen HH, Nguyen HN, Do HD, Pham NTV. Intensity dependence of the Coulomb-repulsion effect in strong-field nonsequential double ionization. *Acta Physica Polonica A*. 2022;141:569-577.
9. Suran VV, Zapesochnyi IP. Observation of Sr<sup>2+</sup> in multiple-photon ionization of strontium. *Soviet Technical Physics Letters*. 1975;1:2.
10. Corkum PB. Plasma perspective on strong field multiphoton ionization. *Physical Review Letters*. 1993;71:1994-7.
11. Ammosov M. V, Delone NB, Krainov VP. Tunnel ionization of complex atoms and of atomic ions in an alternating electromagnetic field. *Soviet Journal of Experimental and Theoretical Physics*. 1986;64:1191.
12. Panfili R, Eberly JH, Haan SL. Comparing classical and quantum dynamics of strong-field double ionization. *Optics Express*. 2001;8:431-435.
13. Haan SL, Breen L, Karim A, Eberly JH. Variable time lag and backward ejection in full-dimensional analysis of strong-field double ionization. *Physical Review Letters*. 2006;97:103008.
14. Zhou Y, Liao Q, Lu P. Asymmetric electron energy sharing in strong-field double ionization of helium. *Physical Review A*. 2010;82:053402.
15. Pham VNT, Tostikhin Oleg I, Morishita T. Molecular Siegert states in an electric field. II. Transverse momentum distribution of the ionized electrons. *Physical Review A*. 2014;89:033426-12.
16. Truong TDH, Nguyen HH, Le HB, Do HD, Tran HM, Nguyen DV, et al. Soft parameters in Coulomb potential of noble atoms for nonsequential double ionization: Classical ensemble model and simulations. *Computer Physics Communications*. 2022;276:108372.
17. Wang X. Theory of strong-field atomic ionization for elliptical or circular polarization [Ph.D. Thesis]. Rochester: University of Rochester; 2013.
18. Benhai Y, Yingbin L. Non-sequential double ionization of argon by elliptically polarized laser pulses. *Journal of Modern Optics*. 2012;59:1797-1802.
19. Chen Y, Zhou Y, Li Y, Li M, Lan P, Lu P. The contribution of the delayed ionization in strong-field nonsequential double ionization. *Journal of Chemical Physics*. 2016;144:024304.
20. Li YB, Wang X, Yu BH, Tang QB, Wang GH, Wan JG. Nonsequential double ionization with mid-infrared laser fields. *Science Reports*. 2016;6:37413.

21. Sarkadi L. Laser-induced nonsequential double ionization of helium: Classical model calculations. *Journal of Physics B*. 2020;53:165401.
22. Eremina E, Liu X, Rottke H, Sandner W, Dreischuh A, Lindner F, et al. Laser-induced non-sequential double ionization investigated at and below the threshold for electron impact ionization. *Journal of Physics B*. 2003;36:3269.